AIMS Mathematics, 10(8): 19940–19957.
DOI:10.3934/math.2025890
Received: 02 July 2025
Revised: 19 August 2025
Accepted: 21 August 2025
Published: 29 August 2025

https://www.aimspress.com/journal/Math

Research article

On incommensurate chaotic fractional discrete model of computer virus: stabilization and synchronization

Omar Kahouli[1,*], Imane Zouak[2], Ma'mon Abu Hammad[3], Adel Ouannas[4] and Mohamed Ayari[5]

[1] Department of Electronics Engineering, Applied College, University of Ha'il, Ha'il 2440, Saudi Arabia

[2] System Dynamics and Control Laboratory, Department of Mathematics and Informatics, University of Larbi Ben M'hidi, Oum El Bouaghi 04000, Algeria

[3] Department of Mathematics, Al-Zaytoonah University of Jordan, Amman 11733, Jordan

[4] Department of Mathematics and Computer Sciences, University of Larbi Ben M'hidi, Oum El Bouaghi 04000, Algeria

[5] Department of Information Technology, Faculty of Computing and Information Technology, Northern Border University, Arar 91431, Saudi Arabia

* **Correspondence:** Email: omarkahouli@yahoo.fr.

Abstract: The chaotic propagation of computer viruses presents a significant challenge in cybersecurity, necessitating advanced mathematical models for understanding and controlling their spread. In this study, we investigate the stabilization and synchronization of chaos in a fractional-order discrete computer virus model with incommensurate order. We begin by analyzing the chaotic behavior of the incommensurate fractional virus model, thereby employing tools such as bifurcation diagrams, phase portraits, and Lyapunov exponents to characterize its nonlinear dynamics. The results reveal that the system exhibits chaotic behavior under specific parameter conditions, which results in unpredictable virus spread. To mitigate these chaotic effects, we implement stabilization strategies aimed at stabilizing the system and suppressing chaotic outbreaks. Additionally, we explore synchronization techniques, which are of paramount importance in understanding virus interactions within networked systems. Numerical results are presented to corroborate the theoretical findings presented in this paper.

Keywords: computer virus model; incommensurate order; chaos; control; synchronization
Mathematics Subject Classification: 34H10, 37N99, 93C55, 93D15, 94C99

1. Introduction

Computer viruses represent a persistent and evolving threat to cybersecurity, thereby impacting digital infrastructure, financial systems, and personal data. These self-replicating malicious programs, which are capable of spreading rapidly across interconnected networks, have become increasingly sophisticated in their methods of evading detection and maintaining persistence within targeted systems. Traditional signature-based and heuristic approaches to combating computer viruses often prove inadequate in addressing the complex and unpredictable nature of virus propagation in today's interconnected world. Consequently, the development of mathematical models has become essential to gain a deeper understanding of virus behavior [1], predict its spread, and devise effective control and mitigation strategies [2–5].

As a framework for non-integer order differentiation and integration, fractional calculus has proven to be a valuable mathematical tool to analyze the behavior of dynamical systems [6, 7]. Unlike conventional models, fractional-order models possess the inherent ability to capture memory effects and hereditary characteristics frequently observed in real-world virus propagation. Specifically, fractional discrete-time models offer a robust framework to investigate how viruses spread within digital systems, where interactions occur at discrete time steps. These models are particularly relevant to cybersecurity due to their capacity to account for the long-term dependencies and adaptive behaviors exhibited by computer viruses.

A crucial distinction within fractional-order models arises between commensurate and incommensurate orders. Commensurate systems are characterized by all fractional derivatives sharing a common base order, whereas incommensurate systems involve multiple, distinct fractional orders. Incommensurate fractional systems are known to exhibit rich and complex dynamics, including chaotic behavior, making their analysis and control particularly challenging [8]. The presence of chaos in computer virus models signifies that seemingly minor variations in the initial states or system parameters can cause drastically different outbreak trajectories, thus significantly complicating prediction and containment efforts [9, 10]. This inherent sensitivity to the initial conditions underscores the critical need for robust control and synchronization techniques to effectively mitigate the chaotic spread of computer viruses [11–14]. To address these challenges, we employ the Caputo-like fractional difference operator, which allows for a tractable analysis in the discrete-time domain. This approach facilitates the decoupling of system memory across compartments with varying fractional orders. Additionally, we apply bifurcation diagrams, a Lyapunov exponent analysis, and entropy measures tailored to incommensurate dynamics, thus ensuring a rigorous investigation of the system behavior under diverse fractional configurations. Modeling such behavior within fractional frameworks helps bridge the gap between theory and practical cybersecurity applications.

Given this potential for chaotic behavior driven by incommensurate orders, developing effective strategies for stabilization and synchronization becomes paramount for practical virus containment. Stabilization involves adaptive strategies to regulate chaotic systems, thus ensuring that the states become asymptotically stable, often converging to equilibrium points. This capability is vital in fields such as robotics, where precise motion control is essential. Despite extensive research on integer-order control, fractional-order control remains largely unexplored due to the complexities of memory effects and non-local dynamics [15, 16]. Synchronization, another critical aspect, was pioneered by Pecora and Carroll, who demonstrated how coupled Lorenz systems can follow identical trajectories [17].

This led to applications in secure communications, which used chaotic signals for encryption. While synchronization is well-studied for integer-order systems [18, 19], fractional-order synchronization presents challenges due to its history-dependent behaviors, necessitating novel techniques [20–32]. In recent years, studies on computer virus propagation have increasingly employed network topology-aware models, such as scale-free and small-world networks [33, 34], to simulate realistic diffusion dynamics and assess control strategies. Alongside these, data-driven methods such as machine learning and deep reinforcement learning have been utilized to predict spread patterns and enhance mitigation efforts [35,36]. However, such models often neglect the long-term memory effects and incommensurate dynamics crucial to accurately describe complex cyber-epidemic phenomena. As a result, existing approaches struggle to accurately capture the complex interplay of discrete events, long-term memory effects, distinct compartment dynamics, and chaotic behavior inherent in real-world computer virus propagation.

Compared to prior studies, our work diverges from existing virus modeling approaches in several key ways. First, most traditional fractional-order cyber-epidemic models (e.g., Wang et al. [37], Yang et al. [38]) operate in a continuous-time setting with fixed structural parameters, whereas our incommensurate discrete-time formulation more accurately mirrors the packet-based and event-driven nature of computer network interactions. Second, machine learning-based prediction and control methods (e.g., Sgandurra et al. [35], Yanfang Ye, et al. [36]) can capture empirical patterns but often function as black boxes, thus overlooking the long-term memory effects and incommensurate dynamics that we explicitly model. Third, unlike commensurate fractional models [39], which assume uniform memory order across all state variables, our framework accommodates distinct fractional orders for each compartment, thus enabling richer dynamics and more realistic propagation scenarios. Finally, although chaos in fractional discrete systems has been generically studied [40], we integrate chaos stabilization and synchronization control directly within the virus modeling framework, which are features largely absent from existing topology-aware or AI-driven studies. This combination of discrete-time incommensurate modeling, explicit chaos control, and integration with stability analyses constitutes the core novelty of our contribution.

Beyond the modeling of virus propagation, chaotic incommensurate systems have gained increasing interest in the field of image encryption, where the unpredictability and sensitivity to the initial conditions are leveraged for security. Notably, recent works have demonstrated how dual discrete memristor-based 3D chaotic maps can be efficiently implemented in multi-channel image encryption [41]. Similarly, parallel color image encryption techniques based on 2D Logistic-Rulkov neuron maps highlight the potential of multi-dimensional chaotic systems for fast and secure encoding processes [42]. These studies illustrate the promising applications of fractional chaotic dynamics in secure communications, this motivating further investigations of such systems in cybersecurity.

In this study, we specifically address the stabilization and synchronization of chaos in a fractional computer virus model with incommensurate orders. Section 2 reviews fundamental concepts of fractional discrete calculus, including notation and stability analyses for fractional maps. Section 3 focuses on the fractional-order computer virus model with incommensurate orders, thereby detailing its dynamics. Section 4 moves the discussion towards the application of advanced stabilization methods, aiming to steer the system toward desirable and stable configurations. We execute nonlinear stability controller procedures to rigorously ensure that the system's trajectories achieve asymptotic convergence to equilibrium points. Section 5 addresses synchronization, thereby providing both

analytical and numerical evidence of error convergence. The paper concludes with Section 6, which provides a summary of the main results and suggests directions for further investigation.

2. Fractional discrete tools

This section establishes the key terms and concepts in discrete fractional calculus. We consider functions defined on $\mathbb{N}_b = \{b, b+1, b+2, \dots\}$, where $b \in \mathbb{R}$.

Definition 1. *[43] For $\varrho(r) : \mathbb{N}_b \to \mathbb{R}$ and $\nu > 0$, the ν-th order fractional sum is given by the following:*

$$\Delta_b^{-\nu}\varrho(r) = \frac{1}{\Gamma(\nu)}\sum_{s=b}^{r-\nu}(r-s-1)^{(\nu-1)}\varrho(s), \quad r \in \mathbb{N}_{b+\nu}, \tag{2.1}$$

where the falling function is defined as

$$r^{(\nu)} = \frac{\Gamma(r+1)}{\Gamma(r+1-\nu)}, \tag{2.2}$$

and $\Gamma(.)$ is Euler's gamma function.

Definition 2. *[44] For ϱ defined on $\mathbb{N}_{b+\delta-\nu}$ and $\nu \notin \mathbb{N}$, the Caputo fractional difference of order ν is as follows:*

$${}^c\Delta_b^{\nu}\varrho(r) = \Delta_b^{-(\delta-\nu)}\Delta^{\delta}\varrho(r) = \frac{1}{\Gamma(\delta-\nu)}\sum_{s=b}^{r-(\delta-\nu)}(r-s-1)^{(\delta-\nu-1)}\Delta^{\delta}\varrho(s), \tag{2.3}$$

for $\delta = \lceil \nu \rceil + 1$.

The theorems presented below are essential for the integrated framework of numerical methods and stability analyses that will be developed for our proposed fractional-order discrete-time system.

Lemme 1. *[45] We examine the following fractional difference equations:*

$$\begin{cases} {}^c\Delta_b^{\nu}\varrho(r) &= f(r+\nu-1, \varrho(r+\nu-1)), \\ \Delta^k\varrho(b) &= \varrho_k, \quad \delta = \lceil \nu \rceil + 1, \quad k = 0, 1, \dots, \delta-1. \end{cases} \tag{2.4}$$

These equations are equivalent to the following discrete integral representation:

$$\varrho(r) = \varrho_0(r) + \frac{1}{\Gamma(\nu)}\sum_{s=b+\delta-\nu}^{r-\nu}(r-s-1)^{(\nu-1)}f(s+\nu-1, \varrho(s+\nu-1)), \tag{2.5}$$

where $r \in \mathbb{N}_{b+\delta}$, and $\varrho_0(r) = \sum_{k=0}^{\delta-1}\frac{(r-b)^{(k)}}{\Gamma(k+1)}\Delta^k\varrho(b)$.

Lemme 2. *[46] Let us consider the following system:*

$$\begin{cases} {}^c\Delta_0^{\nu_1}\varrho_1(r) = \chi_1(\varrho(r+\nu_1-1)), \\ {}^c\Delta_0^{\nu_2}\varrho_2(r) = \chi_2(\varrho(r+\nu_2-1)), \\ \vdots \\ {}^c\Delta_0^{\nu_m}\varrho_m(r) = \chi_m(\varrho(r+\nu_m-1)), \end{cases} \tag{2.6}$$

where $\chi = (\chi_1, \chi_2, ..., \chi_m) : \mathbb{R}^m \to \mathbb{R}^m$, and $\varrho(r) = (\varrho_1(r), \varrho_2(r), ..., \varrho_m(r))^T \in \mathbb{R}^m$. Define M as the least common multiple (LCM) of the denominators u_j of ν_j, where $\nu_j = \frac{v_j}{u_j}$, with $(v_j, u_j) = 1$ and $v_j, u_j \in \mathbb{Z}^+$ for $j = 1, 2, \ldots, m$. Let $w = \frac{1}{M}$; then,

$$\det\left(\text{diag}(\lambda^{M\nu_1}, \lambda^{M\nu_2}, \ldots, \lambda^{M\nu_n}) - (1 - \lambda^M)\mathcal{J}\right) = 0, \tag{2.7}$$

where $\mathcal{J}$ is the Jacobian matrix of (2.6). If all roots of (2.7) are contained within the stability region $\mathbb{C}/O^w$, then the solution of the system (2.6) exhibits local asymptotic stability, where

$$O^w = \left\{ s \in \mathbb{C} : |s| \leq \left(2\cos\frac{|\arg(s)|}{w}\right)^w, \quad \text{and} \quad |\arg(s)| \leq \frac{w\pi}{2} \right\}. \tag{2.8}$$

3. The computer virus model

Building upon the framework established by Ansari et al. [47], this paper introduces a new fractional discrete computer virus propagation model, which is formulated using the Caputo-like operator ${}^c\Delta_b^{\nu_i}, i = 1, 2, 3$, and presents a detailed analyses as follows:

$$\begin{cases} {}^c\Delta_b^{\nu_1} S(n) = \alpha - \beta I(n + \nu_1 - 1)Z(n + \nu_1 - 1) - \mu S(n + \nu_1 - 1), \\ {}^c\Delta_b^{\nu_2} I(n) = \beta I(n + \nu_2 - 1)Z(n + \nu_2 - 1) - \gamma I(n + \nu_2 - 1) - \mu I(n + \nu_2 - 1), \\ {}^c\Delta_b^{\nu_3} Z(n) = \dfrac{1}{\delta}\left(S(n + \nu_3 - 1) - Z(n + \nu_3 - 1)\right), \end{cases} \tag{3.1}$$

The model considers three state variables:

- $S(n)$: the proportion of susceptible (uninfected) computers at time step n;
- $I(n)$: the proportion of infected (virus-carrying) computers at time step n;
- $Z(n)$: the proportion of malicious codes or virus copies circulating in the network at time step n,

where $\nu_i, i = 1, 2, 3$, is the fractional orders. Moreover, it also involves five positive parameters, which are described in Table 1.

Table 1. Descriptions of parameters used in the model.

Parameter	Description
α	Connection rate
β	Infection rate
γ	Recovery rate
μ	Removal rate
δ	Information delay and memory length

This modeling framework is inspired by real-world scenarios that involve the spread of malicious software such as worms (e.g., Conficker) or targeted cyberattacks (e.g., Stuxnet). In this context, S represents the proportion of susceptible (uninfected) systems, I represents the infected systems actively spreading the virus, and Z represents either auxiliary systems or control measures, β represents the infection rate, and T represents the average delay or persistence. The model aids in analyzing infection

peaks, evaluating containment strategies, and designing robust cyber-defense mechanisms. Therefore, it provides not only theoretical insights but also guidance for practical cybersecurity solutions.

Setting $b = 0$, Lemma 1 leads to the following numerical formulas for (3.1):

$$\begin{cases} S(n) = S(0) + \frac{1}{\Gamma(\nu_1)} \sum_{j=1}^{n} \frac{\Gamma(n-j+\nu_1)}{\Gamma(n-j+1)} [\alpha - \beta I(j-1)Z(j-1) - \mu S(j-1)], \\ I(n) = I(0) + \frac{1}{\Gamma(\nu_2)} \sum_{j=1}^{n} \frac{\Gamma(n-j+\nu_2)}{\Gamma(n-j+1)} [\beta I(j-1)Z(j-1) - \gamma I(j-1) - \mu I(j-1)], \\ Z(n) = Z(0) + \frac{1}{\Gamma(\nu_3)} \sum_{j=1}^{n} \frac{\Gamma(n-j+\nu_3)}{\Gamma(n-j+1)} [\frac{1}{\delta}(S(j-1) - Z(j-1))]. \end{cases} \tag{3.2}$$

The initial states of the system are represented by $S(0)$, $I(0)$, and $Z(0)$.

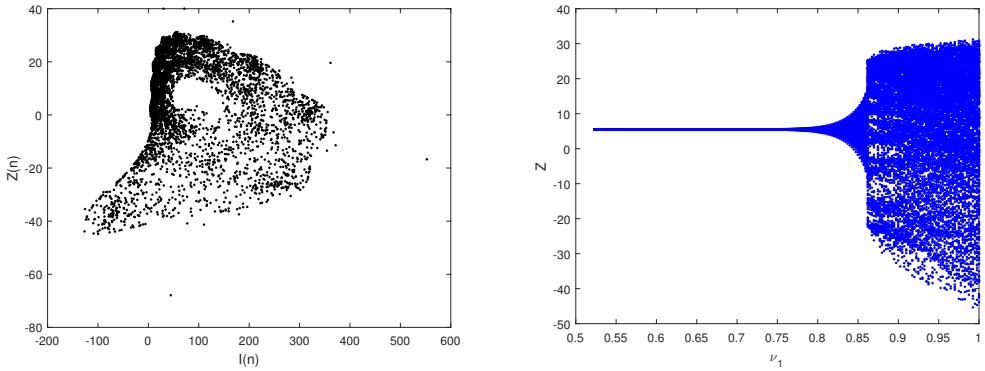

(a) $(\nu_1, \nu_2, \nu_3) = (0.99, 0.95, 0.75)$ **(b)** $(\nu_2, \nu_3) = (0.95, 0.75)$

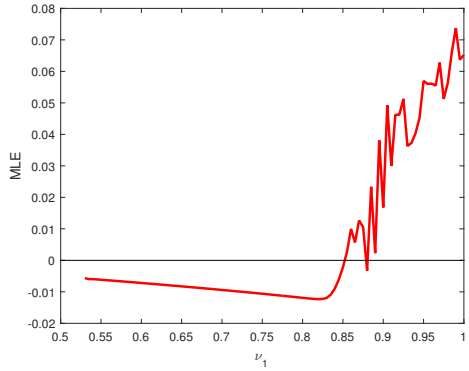

(c) $(\nu_2, \nu_3) = (0.95, 0.75)$

Figure 1. Phase portrait, bifurcation diagram, and the corresponding Maximum Lyapunov Exponent (MLE) for system (3.1): (a) phase portrait for $(\nu_1, \nu_2, \nu_3) = (0.99, 0.95, 0.75)$; (b) bifurcation diagram concerning ν_1 for fixed $(\nu_2, \nu_3) = (0.95, 0.75)$; (c) MLE plot corresponding to (b).

Before introducing stabilization and synchronization strategies for the fractional model (3.1), we need to examine its fundamental dynamics. For this purpose, we begin with the specific case where $S(0) = 40$, $I(0) = 30$, and $Z(0) = 40$. Figure 1 provides a compelling visualization of the complex dynamics exhibited by the incommensurate fractional-order discrete-time system (3.1) by utilizing the parameter values $(\alpha, \beta, \gamma, \mu, \delta) = (20, 0.04, 0.02, 0.2, 7.5)$. These values were selected based on extensive numerical experiments using MATLAB; they were found to produce complex and chaotic

dynamics, which are central to the objective of the study. The phase portraits are displayed in Figure 1(a), which reveals a chaotic attractor, suggesting complex and irregular system behavior. This observation is reinforced by the bifurcation diagram in Figure 1(b), which eloquently captures the transition from stable and periodic behavior at lower parameter values ν_1 to chaotic dynamics as the control parameter ν_1 increases. The cascade of bifurcations leading to chaos is a classic signature of nonlinear systems. Further solidifying this analysis, the Maximum Lyapunov Exponent (MLE) plot provides a quantitative measure of the system's chaoticity: using the Jacobian matrix method [48], the positive MLE values observed at higher ν_1 values confirm the presence of chaos, with the fluctuations suggesting varying degrees of chaotic intensity. The combination of these three graphical representations-phase portrait, bifurcation diagram, and MLE plot-offers a comprehensive and insightful portrayal of the system's motion, thus underscoring the intricate interplay of parameters and the emergence of chaos in this fractional discrete-time model of computer viruses. In conclusion, this figure effectively communicates the rich and complex dynamics inherent in this fractional discrete-time system, thereby highlighting the emergence of chaos and the role of incommensurability in shaping its behavior.

4. Stabilization of chaos

A key aspect of studying chaotic dynamical systems is the ability to control or stabilize them. In this context, stabilization involves introducing adaptive terms to the system to asymptotically drive its states to the fixed point. Note that this model (3.1) has two equilibrium points, $E_0 = (\frac{b}{\mu}, 0, \frac{b}{\mu})$ and $E^* = (S^*, I^*, Z^*)$, where

$$S^* = \frac{\gamma+\mu}{\beta}, \quad I^* = \frac{\alpha}{\gamma+\mu} - \frac{\mu}{\beta}, \quad Z^* = \frac{\gamma+\mu}{\beta}. \tag{4.1}$$

4.1. Stabilizing E_0

To stabilize the 3D proposed incommensurate model (3.1), we derive a stability requirement that guarantees the convergence of all states to the free fixed point E_0. Theorem 1 is employed in this analysis.

The following equations describe the controlled model of incommensurate order:

$$\begin{cases} {}^c\Delta_b^{\nu_1} S(n) = \alpha - \beta I(n+\nu_1-1)Z(n+\nu_1-1) - \mu S(n+\nu_1-1) + C_1(n+\nu_1-1), \\ {}^c\Delta_b^{\nu_2} I(n) = \beta I(n+\nu_2-1)Z(n+\nu_2-1) - \gamma I(n+\nu_2-1) - \mu I(n+\nu_2-1) + C_2(n+\nu_2-1), \\ {}^c\Delta_b^{\nu_3} Z(n) = \frac{1}{\delta}(S(n+\nu_3-1) - Z(n+\nu_3-1)) + C_3(n+\nu_3-1). \end{cases} \tag{4.2}$$

Theorem 1. *A three-dimensional control law is designed with the specific objective of stabilizing the dynamics of the incommensurate model* (3.1) *as follows:*

$$\begin{cases} C_1(n) = c_1(\frac{\alpha}{\mu} - S(n)) + \beta I(n)Z(n), \\ C_2(n) = c_2 I(n) - \beta I(n)Z(n), \\ C_3(n) = c_3(\frac{\alpha}{\mu} - Z(n)), \end{cases} \tag{4.3}$$

with $c_1 = 0.89, c_2 = -0.79$, and $c_3 = 0.92$.

Proof: Substituting (4.3) into (4.2) yields the following:

$$\begin{cases} {}^{c}\Delta_b^{\nu_1} S(n) = \alpha - \mu S(n+\nu_1-1) + c_1(\frac{\alpha}{\mu} - S(n+\nu_1-1)), \\ {}^{c}\Delta_b^{\nu_2} I(n) = -\gamma I(n+\nu_2-1) - \mu I(n+\nu_2-1) + c_2 I(n+\nu_2-1)), \\ {}^{c}\Delta_b^{\nu_3} Z(n) = \frac{1}{\delta}(S(n+\nu_3-1) - Z(n+\nu_3-1)) + c_3(\frac{\alpha}{\mu} - Z(n+\nu_3-1)). \end{cases} \tag{4.4}$$

Then,

$$\det\left(\text{diag}(\lambda^{M\nu_1}, \lambda^{M\nu_2}, \lambda^{M\nu_3}) - (1-\lambda^M)\mathcal{H}\right) = 0. \tag{4.5}$$

For $(\nu_1, \nu_2, \nu_3) = (0.89, 0.95, 0.75)$, we get $M = 100$, and

$$\det\left(\begin{pmatrix} \lambda^{89} & 0 & 0 \\ 0 & \lambda^{95} & 0 \\ 0 & 0 & \lambda^{75} \end{pmatrix} - (1-\lambda^{100})\mathcal{H}\right) = 0, \tag{4.6}$$

where the controlled system's Jacobian for the previous parameters leading to chaos $\delta = 7.5, \gamma = 0.02, \beta = 0.04, \mu = 0.2, \alpha = 20$, and $c_1 = 0.89, c_2 = -0.79$, and $c_3 = 0.92$, is

$$\mathcal{H} = \begin{pmatrix} -1.09 & 0 & 0 \\ 0 & -1.01 & 0 \\ \frac{1}{7.5} & 0 & -\frac{79}{75} \end{pmatrix}. \tag{4.7}$$

The control gains $c_1 = 0.89, c_2 = -0.79$, and $c_3 = 0.92$ were systematically optimized to satisfy the stability conditions of Lemma 2 for the incommensurate system. Through a parametric sensitivity analysis, we determined these values ensure that all characteristic roots of Eq (4.5) lie strictly outside $O^{\frac{1}{100}}$, thus guaranteeing asymptotic stability. Their effectiveness was further confirmed through simulations.

The characteristic equation is given by the following:

$$\left(\lambda^{75} - \frac{79}{75}\lambda^{100} + \frac{79}{75}\right)(\lambda^{95} - 1.01\lambda^{100} + 1.01)(\lambda^{89} - 1.09\lambda^{100} + 1.09) = 0. \tag{4.8}$$

We seek to prove that the asymptotic stability of E_0, thereby guaranteeing the convergence of all states to E_0 in the long run. Equation (4.8) has 300 solutions, $\lambda_j (j = 1, ..., 300)$, all of which lie in $\mathbb{C}/O^{\frac{1}{100}}$. By Lemma 2, system (4.2) is locally asymptotically stable to the free fixed point $E_0 = (\frac{\alpha}{\mu}, 0, \frac{\alpha}{\mu})$.

We numerically verified the results of Theorem 1 using MATLAB. The discrete-time states, as illustrated in Figure 2, confirm the system's asymptotic stability, with all states converging to E_0.

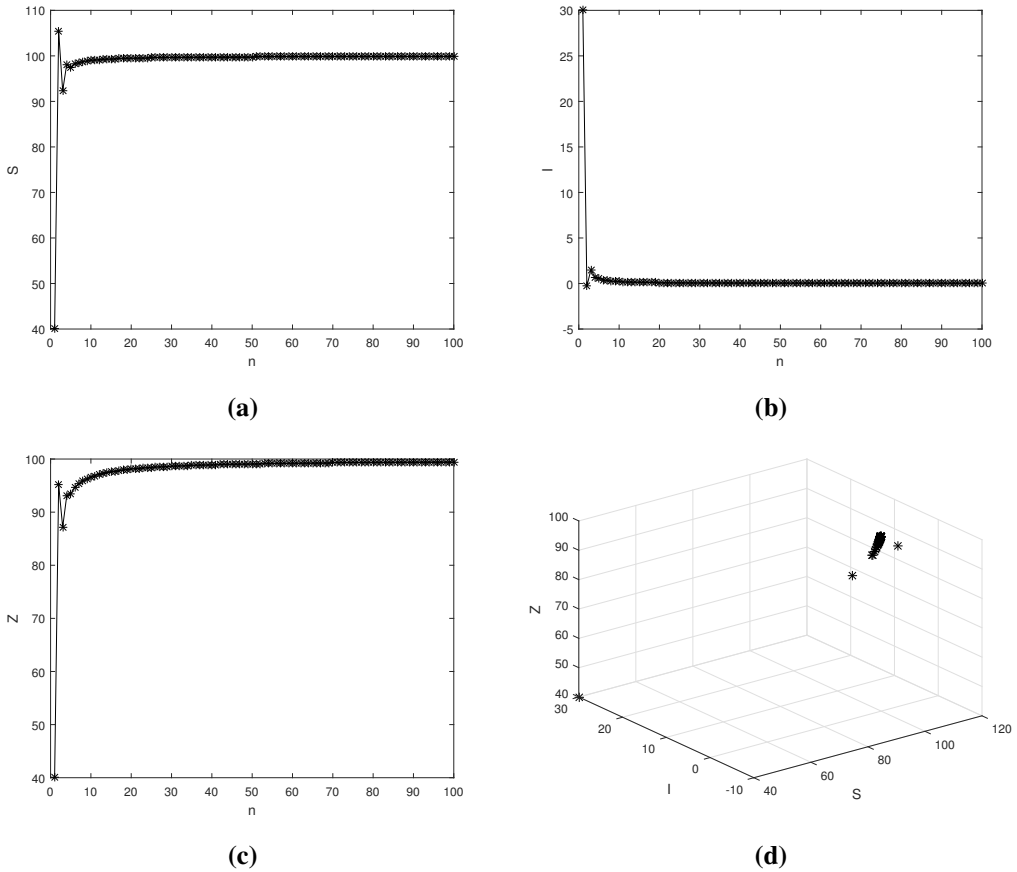

(a) **(b)** **(c)** **(d)**

Figure 2. Stabilization of (3.1) to E_0 for $(\nu_1, \nu_2, \nu_3) = (0.89, 0.95, 0.75)$.

4.2. Stabilizing E^*

Now, we will construct adaptive laws that will effectively stabilize the fractional model (3.1), thus forcing all of its states to asymptotically approach E^*. To manage the dynamics of the incommensurate model, we introduce the following control mechanism:

$$\begin{cases} {}^{c}\Delta_{b}^{\nu_1} S(n) = \alpha - \beta I(n+\nu_1-1)Z(n+\nu_1-1) - \mu S(n+\nu_1-1) + \mathcal{F}_1(n+\nu_1-1), \\ {}^{c}\Delta_{b}^{\nu_2} I(n) = \beta I(n+\nu_2-1)Z(n+\nu_2-1) - \gamma I(n+\nu_2-1) - \mu I(n+\nu_2-1) + \mathcal{F}_2(n+\nu_2-1), \\ {}^{c}\Delta_{b}^{\nu_3} Z(n) = \frac{1}{\delta}(S(n+\nu_3-1) - Z(n+\nu_3-1)) + \mathcal{F}_3(n+\nu_3-1). \end{cases} \tag{4.9}$$

Theorem 2 creates the control law for the stabilization of the incommensurate model in the direction of E^*.

Theorem 2. *We construct a control law in the following manner:*

$$\begin{cases} \mathcal{F}_1(n) = f_1(S^* - S(n)) + \beta I(n)Z(n), \\ \mathcal{F}_2(n) = f_2(I^* - I(n)) - \beta I(n)Z(n), \\ \mathcal{F}_3(n) = f_3(Z^* - Z(n)) - \frac{1}{T}S(n), \end{cases} \tag{4.10}$$

where $f_1 = 0.89$, $f_2 = 0.79$, and $f_3 = 0.92$, are constant control gains. Then, the stabilization of the incommensurate model (3.1) to the E^* equilibrium is achieved.

Proof: Substituting (4.10) into (4.9) gives the following

$$\begin{cases} {}^{c}\Delta_{b}^{\nu_1} S(n) = \alpha - \mu S(n+\nu_1-1) + f_1(S^* - S\,nr)), \\ {}^{c}\Delta_{b}^{\nu_2} I(n) = -\gamma I(n+\nu_2-1) - \mu I(n+\nu_2-1) + f_2(I^* - I(n)), \\ {}^{c}\Delta_{b}^{\nu_3} Z(n) = -\frac{1}{\delta} Z(n+\nu_3-1) + f_3(Z^* - Z(n)). \end{cases} \tag{4.11}$$

For brevity, we follow the same procedure as in the proof of Theorem 1. First, we derive the corresponding characteristic equation and analyze the location of its roots:

$$\left(\lambda^{75} - \frac{79}{75}\lambda^{100} + \frac{79}{75}\right)(\lambda^{95} - 1.01\lambda^{100} + 1.01)(\lambda^{89} - 1.09\lambda^{100} + 1.09) = 0. \tag{4.12}$$

All 300 solutions of Eq (4.12), $\lambda_j (j = 1, ..., 300)$, lie within $\mathbb{C}/O^{\frac{1}{100}}$. As a result, (4.9) is asymptotically stable in the direction of E^*. The control coefficients $f_1 = 0.89$, $f_2 = 0.79$, and $f_3 = 0.92$ were determined through a structured parameter search coupled with stability verification based on Lemma 2. For each candidate set of gains, the characteristic roots of Eq (4.12) were computed, and only those that satisfied the stability conditions of Lemma 2 were retained. This procedure ensured that the selected gains provide sufficient negative feedback to suppress chaotic oscillations, while guaranteeing asymptotic stability of the incommensurate fractional-order system around the equilibrium point E^*.

The validity of Theorem 2 was assessed through a numerical simulation that used the specified parameters, initial conditions, and control laws in Figure 1. The time evolution of the states, as visually represented in Figure 3, provides clear evidence of convergence to E^*, thus demonstrating successful stabilization.

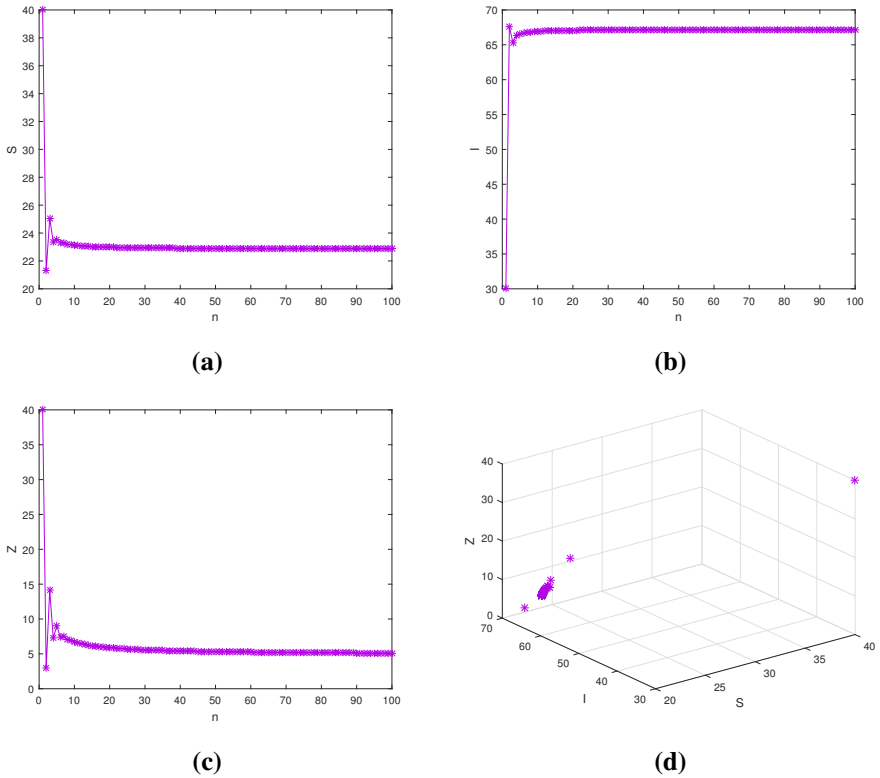

(a) **(b)** **(c)** **(d)**

Figure 3. Stabilization of (3.1) to E^* for $(\nu_1, \nu_2, \nu_3) = (0.89, 0.95, 0.75)$.

5. Chaos synchronization

We aim to synchronize fractional discrete models by minimizing the discrepancy between a master and slave model. The master model is defined using the incommensurate fractional computer model (3.1). Then, we specify the slave model as follows:

$$\begin{cases} {}^{c}\Delta_{b}^{\nu_1} S_m(n) = \alpha - \beta I_m(n+\nu_1-1) Z_m(n+\nu_1-1) - \mu S_m(n+\nu_1-1), \\ {}^{c}\Delta_{b}^{\nu_2} I_m(n) = \beta I_m(n+\nu_2-1) Z_m(n+\nu_2-1) - \gamma I_m(n+\nu_2-1) - \mu I_m(n+\nu_2-1), \\ {}^{c}\Delta_{b}^{\nu_3} Z_m(n) = \frac{1}{\delta}(S_m(n+\nu_3-1) - Z_m(n+\nu_3-1)). \end{cases} \tag{5.1}$$

The respective slave system is the following:

$$\begin{cases} {}^{c}\Delta_{b}^{\nu_1} S_s(n) = \alpha - \beta I_s(n+\nu_1-1) Z_s(n+\nu_1-1) - \mu S_s(n+\nu_1-1) + \mathcal{T}_1(n+\nu_1-1), \\ {}^{c}\Delta_{b}^{\nu_2} I_s(n) = \beta I_s(n+\nu_2-1) Z_s(n+\nu_2-1) - \gamma I_s(n+\nu_2-1) - \mu I_s(n+\nu_2-1) + \mathcal{T}_2(n+\nu_2-1), \\ {}^{c}\Delta_{b}^{\nu_3} Z_s(n) = \frac{1}{\delta}(S_s(n+\nu_3-1) - Z_s(n+\nu_3-1)) + \mathcal{T}_3(n+\nu_3-1). \end{cases} \tag{5.2}$$

Master-slave system synchronization (Eqs (5.1) and (5.2)) occurs when the controllers $\mathcal{T}_i (i = 1, ..., 3)$ ensure asymptotic convergence of the synchronization errors to zero as follows:

$$\begin{cases} {}^{c}\Delta_{b}^{\nu_1} e_1(n) = & -\beta(I_s(n+\nu_1-1) Z_s(n+\nu_1-1) - I_m(n+\nu_1-1) Z_m(n+\nu_1-1)) \\ & -\mu(S_s(n+\nu_1-1) - S_m(n+\nu_1-1)) + \mathcal{T}_1(n+\nu_1-1), \\ {}^{c}\Delta_{b}^{\nu_2} e_2(n) = & \beta(I_s(n+\nu_2-1) Z_s(n+\nu_2-1) - I_m(n+\nu_2-1) Z_m(n+\nu_2-1)) \\ & -\gamma(I_s(n+\nu_2-1) - I_m(n+\nu_2-1)) - \mu(I_s(n+\nu_2-1) - I_m(n+\nu_2-1)) + \mathcal{T}_2(n+\nu_2-1), \\ {}^{c}\Delta_{b}^{\nu_3} e_3(n) = & \frac{1}{\delta}(S_s(n+\nu_3-1) - S_m(n+\nu_3-1) - Z_s(n+\nu_3-1) + Z_m(n+\nu_3-1)) + \mathcal{T}_3(n+\nu_3-1). \end{cases} \tag{5.3}$$

Theorem 3 presents adaptive rules for the controllers $\mathcal{T}_i (i = 1, ..., 3)$, to ensure that the synchronization error tends asymptotically towards zero.

Theorem 3. *Subject to the following:*

$$\begin{cases} \mathcal{T}_1(n+\nu_1-1) = \beta(I_s(n+\nu_1-1) Z_s(n+\nu_1-1) - I_m(n+\nu_1-1) Z_m(n+\nu_1-1)) + t_1 e_1(n+\nu_1-1), \\ \mathcal{T}_2(n+\nu_2-1) = -\beta(I_s(n+\nu_2-1) Z_s(n+\nu_2-1) - I_m(n+\nu_2-1) Z_m(n+\nu_2-1)) + t_2 e_2(n+\nu_2-1), \\ \mathcal{T}_3(n+\nu_3-1) = t_3 e_3(n+\nu_3-1). \end{cases} \tag{5.4}$$

Synchronization is realized among the master system (5.1) and the slave systems (5.2), for $t_1 = -0.35, t_2 = -0.51$, and $t_3 = -0.8$.

Proof: The error dynamics are derived by first applying the fractional difference operator to the synchronization errors in Eq (5.3) and subsequently substituting the proposed controllers (5.4) as follows:

$$\begin{cases} {}^{c}\Delta_{b}^{\nu_1} e_1(n) = -\mu e_1(n+\nu_1-1) + t_1 e_1(n+\nu_1-1), \\ {}^{c}\Delta_{b}^{\nu_2} e_2(n) = -\mu e_2(n+\nu_2-1) - \gamma e_2(n+\nu_2-1) + t_2 e_2(n+\nu_2-1), \\ {}^{c}\Delta_{b}^{\nu_3} e_3(n) = \frac{1}{\delta}(e_1(n+\nu_3-1) - e_3(n+\nu_3-1)) + t_3 e_3(n+\nu_3-1). \end{cases} \tag{5.5}$$

Thus,

$$\det\left(\text{diag}(\lambda^{M\nu_1}, \lambda^{M\nu_2}, \lambda^{M\nu_3}) - (1-\lambda^M)\mathcal{L}\right) = 0. \tag{5.6}$$

To avoid redundancy, we adopt the same methodology as used in the proof of Theorem 1. Specifically, we construct the characteristic equation and examine the root conditions to establish stability as follows:

$$\left(\lambda^{75} - \frac{14}{15}\lambda^{100} + \frac{14}{15}\right)(\lambda^{95} - 0.73\lambda^{100} + 0.73)(\lambda^{89} - 0.55\lambda^{100} + 0.55) = 0. \tag{5.7}$$

The 300 solutions, $\lambda_j (j = 1, ..., 300)$, of Eq (5.7), lie in $\mathbb{C}/O^{\frac{1}{100}}$. Fast convergence of the errors in (5.3) to zero is necessary for synchronization. Because matrix $\mathcal{L}$ meets the stability condition of Lemma 2, the error system (5.3) is asymptotically stable, thus leading to the synchronization of systems (5.1) and (5.2).

To illustrate the effectiveness of the synchronization scheme proposed in Theorem 3, we numerically simulate the error dynamics governed by system (5.3) using the parameters defined previously with $(\nu_1, \nu_2, \nu_3) = (0.89, 0.95, 0.75)$.

Figure 4 displays the evolution of the synchronization errors for four distinct sets of initial conditions, which were selected to represent both small and large deviations from the equilibrium state. In all cases, the error trajectories monotonically converge toward zero, thus confirming the robustness of the proposed synchronization scheme against variations in the initial state of the master and slave systems. This consistent convergence across multiple scenarios demonstrates that the control law is not limited to specific initial configurations but ensures global-like synchronization within the tested parameter domain.

It is important to note that numerical solutions of fractional-order discrete systems may be subject to the accumulation of truncation and round-off errors over long iterations, due to the memory effect inherent in fractional differences. In our simulations, we mitigated this by employing double-precision arithmetic and verifying the convergence consistency when either reducing the step size or increasing the computation precision. The resulting numerical deviations were found to be negligible and did not alter the qualitative synchronization behavior presented in Figure 4.

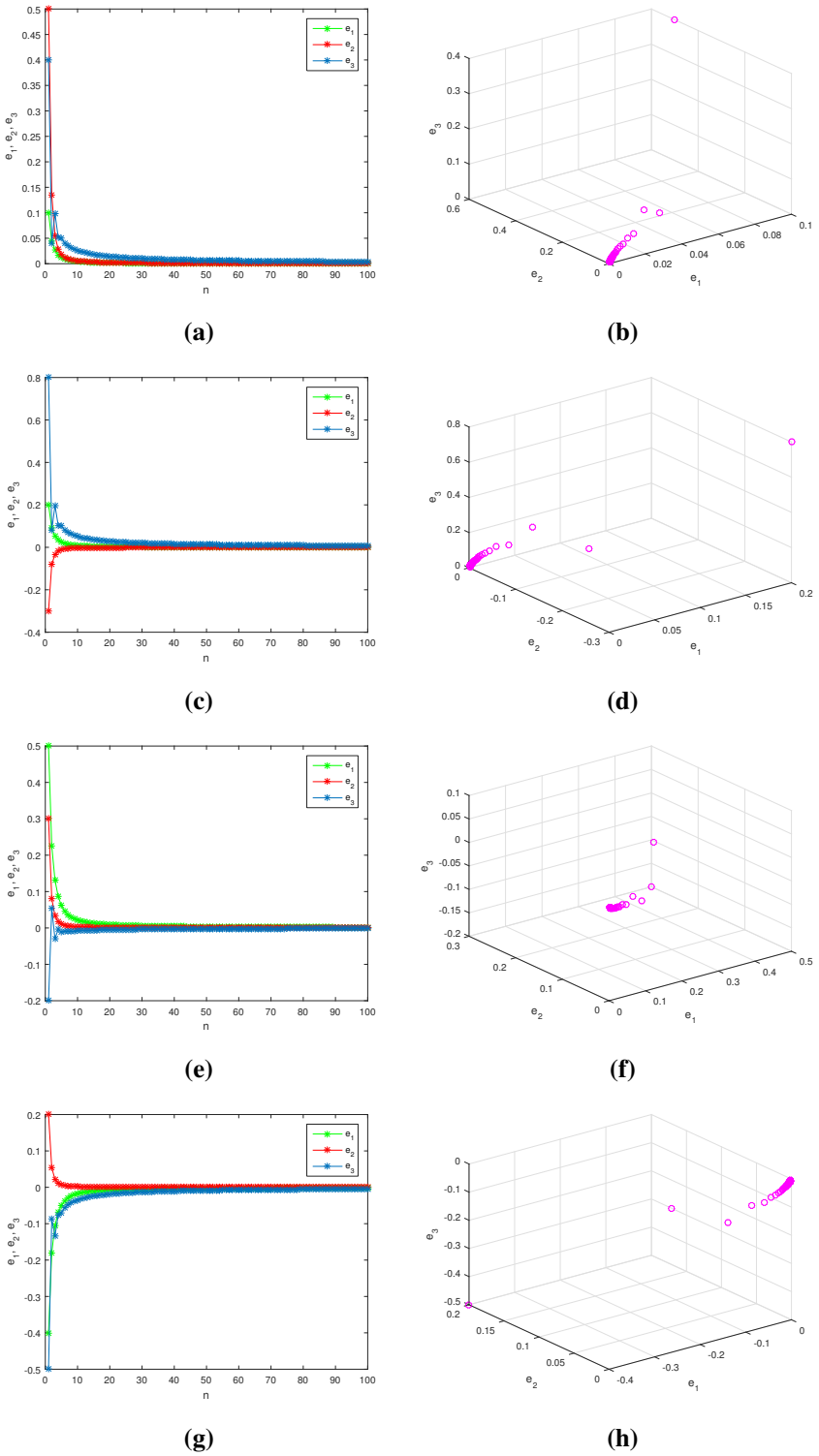

Figure 4. Evolution of the synchronization errors (5.3): (a), (b) for $(e_1(0), e_2(0), e_3(0)) = (0.1, 0.5, 0.4)$; (c), (d) for $(e_1(0), e_2(0), e_3(0)) = (0.2, -0.3, 0.8)$; (e), (f) for $(e_1(0), e_2(0), e_3(0)) = (0.5, 0.3, -0.2)$; (g), (h) for $(e_1(0), e_2(0), e_3(0)) = (-0.4, 0.2, -0.5)$.

6. Conclusions and perspectives

This research delved into the intricate state space of chaos in a fractional-order discrete computer virus model with incommensurate orders, thereby exploring both stabilization and synchronization strategies. Through bifurcation diagrams, Lyapunov exponents, and phase portraits, we identified chaotic behavior under specific parameter conditions, thus emphasizing the unpredictability of virus spread and the need for effective mitigation techniques. To this end, we proposed control mechanisms to stabilize two key equilibria: the virus-free equilibrium E_0 and the endemic state E^*. Both strategies successfully suppressed chaos, thereby demonstrating their potential to regulate erratic viral dynamics. In addition, synchronization methods were introduced to model virus behavior in interconnected systems, thus providing valuable insights for managing propagation in networked environments.

Beyond virus modeling, the developed control and synchronization strategies for chaotic incommensurate discrete-time systems hold significant promise for broader applications in cryptography, information security, and secure communication systems. Recent studies have demonstrated how such systems can enhance encryption robustness and computational efficiency, which were exemplified by 3D memristive maps with dual discrete memristors [41] and 2D logistic Rulkov neuron-based parallel image encryption schemes [42]. Additionally, Gao et al. [49] introduced a three-dimensional memristor-based hyperchaotic map tailored for pseudorandom number generation and multi-image encryption. This model systematically evaluates the chaotic characteristics and encryption performance, thereby offering a valuable point of comparison and complementing our incommensurate-order system in terms of high-dimensional chaotic dynamics and parallel encryption capabilities. These applications collectively underscore the potential of our fractional chaotic framework to advance cybersecurity solutions.

Future work will focus on validating the model's practical relevance through simulations based on real virus propagation datasets and realistic network structures such as small-world, scale-free, and random topologies. This will enable the assessment of the model's performance in practical cybersecurity environments and guide its application in mitigating real threats. Additionally, we plan to investigate adaptive and hybrid control strategies that dynamically respond to changing virus patterns, including the effects of time delays and multi-layered network interactions. Moreover, future efforts will explore interdisciplinary applications of the proposed framework in evolving cybersecurity contexts, including anomaly detection, predictive defense models, and data-driven strategies for virus containment.

Author contributions

Omar Kahouli: methodology, funding acquisition, project administration, validation; Imane Zouak: conceptualization, methodology, software, formal analysis, data curation, writing original draft preparation, writing review and editing, investigation, visualization; Ma'mon Abu Hammad: Project administration, funding acquisition, visualization, resources; Adel Ouannas: conceptualization, supervision, visualization, resources, validation; Mohamed Ayari: project administration, validation, resources. All authors have read and approved the final version of the manuscript for publication.

Use of Generative-AI Tools Declaration

The authors declare that no generative Artificial Intelligence (AI) tools were used in the creation of this article.

Acknowledgments

The authors extend their appreciation to the Deanship of Scientific Research at Northern Border University, Arar, KSA, for funding this research work through the project number (NBU-FPEJ-2025-2443-05).

Conflict of interest

The authors declare that there are no conflicts of interest regarding the publication of this paper.

References

1. P. Szor, *The art of computer virus research and defense*, 1 Eds., Massachusetts: Addison-Wesley Professional, 2005.
2. X. F. Yang, L.-X. Yang, Towards the epidemiological modeling of computer viruses, *Discrete Dyn. Nat. Soc.*, **2012** (2012), 259671. https://doi.org/10.1155/2012/259671
3. J. G. Ren, X. F. Yang, Q. Y. Zhu, L.-X. Yang, C. M. Zhang, A novel computer virus model and its dynamics, *Nonlinear Anal.-Real*, **13** (2012), 376–384. https://doi.org/10.1016/j.nonrwa.2011.07.048
4. L.-X. Yang, X. F. Yang, Q. Y. Zhu, L. S. Wen, A computer virus model with graded cure rates, *Nonlinear Anal.-Real*, **14** (2013), 414–422. https://doi.org/10.1016/j.nonrwa.2012.07.005
5. L.-X. Yang, X. F. Yang, A new epidemic model of computer viruses, *Commun. Nonlinear Sci.*, **19** (2014), 1935–1944. https://doi.org/10.1016/j.cnsns.2013.09.038
6. G. C. Wu, D. Baleanu, Discrete fractional logistic map and its chaos, *Nonlinear Dyn.*, **75** (2014), 283–287. https://doi.org/10.1007/s11071-013-1065-7
7. M. Al-Qurashi, Q. U. Asif, Y.-M. Chu, S. Rashid, S. K. Elagan, Complexity analysis and discrete fractional difference implementation of the Hindmarsh–Rose Neuron System, *Results Phys.*, **51** (2023), 106627. https://doi.org/10.1016/j.rinp.2023.106627
8. I. H. Jebril, K. Dibi, I. Zouak, A. Ouannas, A.-A. Khennaoui, I. M. Batiha, Incommensurate fractional computer virus system: control and simulation, *2025 12th International Conference on Information Technology (ICIT)*, Amman, Jordan, 2025, 109–113. https://doi.org/10.1109/ICIT64950.2025.11049232
9. O. Kahouli, I. Zouak, M. A. Hammad, A. Ouannas, Chaos, control, and synchronization in discrete time computer virus system with fractional orders, *AIMS Mathematics*, **10** (2025), 13594–13621. http://doi.org/10.3934/math.2025612

10. J. Oudetallah, I. Zouak, W. Audeh, A. Ouannas, A.-A. Khennaoui, I. M. Batiha, S. Momani, Control of chaos in fractional computer virus model, *2025 1st International Conference on Computational Intelligence Approaches and Applications (ICCIAA)*, Amman, Jordan, 2025, 01–05. https://doi.org/10.1109/ICCIAA65327.2025.11013727

11. O. Kahouli, I. Zouak, A. Ouannas, I. Abidi, Y. Bahou, S. Elgharbi, et al., Control and synchronization of chaos in some fractional computer virus models, *Asian J. Control*, **2025** (2015), 1–9. https://doi.org/10.1002/asjc.3693

12. J. Oudetallah, I. Zouak, W. Audeh, A. Ouannas, A.-A. Khennaoui, I. M. Batiha, et al., Synchronization of computer virus system using fractional calculus, *2025 1st International Conference on Computational Intelligence Approaches and Applications (ICCIAA)*, Amman, Jordan, 2025, 1–6. https://doi.org/10.1109/ICCIAA65327.2025.11013551

13. A.-A. Khennaoui, A. Ouannas, S. Bendoukha, X. Wang, V. T. Pham, On chaos in the fractional-order discrete-time unified system and its control synchronization, *Entropy*, **20** (2018), 530. https://doi.org/10.3390/e20070530

14. A. O. Almatroud, A.-A. Khennaoui, A. Ouannas, G. Grassi, M. M. Al-Sawalha, A. Gasri, Dynamical analysis of a new chaotic fractional discrete-time system and its control, *Entropy*, **22** (2020), 1344. https://doi.org/10.3390/e22121344

15. L. M. Pecora, T. L. Carrol, Synchronization in chaotic systems, *Phys. Rev. Lett.*, **64** (1990), 821. https://doi.org/10.1103/PhysRevLett.64.821

16. A. Ouannas, Z. Odibat, Generalized synchronization of different dimensional chaotic dynamical systems in discrete-time, *Nonlinear Dyn.*, **81** (2015), 765–771. https://doi.org/10.1007/s11071-015-2026-0

17. A. Ouannas, A new generalized type of synchronization for discrete chaotic dynamical systems, *J. Comput. Nonlinear Dynam.*, **10** (2015), 061019. https://doi.org/10.1115/1.4030295

18. A. Gasri, A. Ouannas, A. A. Khennaoui, G. Grassi, T. Oussaeif, V. T. Pham, Chaotic fractional discrete neural networks based on the Caputo h-difference operator: stabilization and linear control laws for synchronization, *Eur. Phys. J. Spec. Top.*, **231** (2022), 1815–1829. https://doi.org/10.1140/epjs/s11734-022-00552-3

19. R. Saadeh, A. Abbes, A. Al-Husban, A. Ouannas, G. Grassi, The fractional discrete predator–prey model: chaos, control and synchronization, *Fractal Fract.*, **7** (2023), 120. https://doi.org/10.3390/fractalfract7020120

20. A. Abbes, A. Ouannas, N. Shawagfeh, G. Grassi, The effect of the Caputo fractional difference operator on a new discrete COVID-19 model, *Results Phys.*, **39** (2022), 105797. https://doi.org/10.1016/j.rinp.2022.105797

21. M. T. Shatnawi, A. Abbes, A. Ouannas, I. M. Batiha, A new two-dimensional fractional discrete rational map: chaos and complexity, *Phys. Scr.*, **98** (2023), 015208. https://doi.org/10.1088/1402-4896/aca531

22. A.-A. Khennaoui, A. Ouannas, S. Momani, O. A. Almatroud, M. M. Al-Sawalha, S. M. Boulaaras, et al., Special fractional-order map and its realization, *Mathematics*, **10** (2022), 4474. https://doi.org/10.3390/math10234474

23. A. Abbes, A. Ouannas, N. Shawagfeh, An incommensurate fractional discrete macroeconomic system: bifurcation, chaos, and complexity, *Chin. Phys. B*, **32** (2023), 030203. https://doi.org/10.1088/1674-1056/ac7296

24. A. Ouannas, I. M. Batiha, V. T. Pham, *Fractional discrete chaos: theories, methods and applications*, Singapore: World Scientific, 2023.

25. T. Hamadneh, A. Abbes, I. Abu Falahah, Y. A. Al-Khassawneh, A. S. Heilat, A. Al-Husban, et al., Complexity and chaos analysis for two-dimensional discrete-time predator–prey Leslie–Gower model with fractional orders, *Axioms*, **12** (2023), 561. https://doi.org/10.3390/axioms12060561

26. O. A. Almatroud, M. Abu Hammad, A. Dababneh, L. Diabi, A. Ouannas, A. A. Khennaoui, et al., Multistability, chaos, and synchronization in novel symmetric difference equation, *Symmetry*, **16** (2024), 1093. https://doi.org/10.3390/sym16081093

27. M. Abu Hammad, L. Diabi, A. Dababneh, A. Zraiqat, S. Momani, A. Ouannas, et al., On new symmetric fractional discrete-time systems: chaos, complexity, and control, *Symmetry*, **16** (2024), 840. https://doi.org/10.3390/sym16070840

28. N. Djenina, A. Ouannas, Stability and stabilisation of nonlinear incommensurate fractional order difference systems, In: *State estimation and stabilization of nonlinear systems*, Cham: Springer, 2023, 147–168. https://doi.org/10.1007/978-3-031-37970-3_9

29. H. Al-Taani, M. Abu Hammad, M. Abudayah, L. Diabi, A. Ouannas, Asymmetry and symmetry in a new three-dimensional chaotic map with commensurate and incommensurate fractional orders, *Symmetry*, **16** (2024), 1447. https://doi.org/10.3390/sym16111447

30. M. Abu Hammad, R. Alkhateeb, G. Farraj, N. Djenina, A. Ouannas, Discrete fractional incommensurate order Ebola model: analyzing dynamics and numerical simulation, *Fractals*, **33** (2025), 2540127. https://doi.org/10.1142/S0218348X25401279

31. A. Ouannas, S. B. Ahmed, G. Grassi, M. Al Horani, A. A. Khennaoui, A. Hioual, The fractional variable-order Grassi–Miller map: chaos, complexity, and control, *Comput. Math. Methods*, **2025** (2025), 6674521. https://doi.org/10.1155/2025/6674521

32. L. Diabi, A. Ouannas, A. Hioual, G. Grassi, S. Momani, The discrete Ueda system and its fractional order version: chaos, stabilization and synchronization, *Mathematics*, **13** (2025), 239. https://doi.org/10.3390/math13020239

33. R. Pastor-Satorras, A. Vespignani, Epidemic spreading in scale-free networks, *Phys. Rev. Lett.*, **86** (2001), 3200. https://doi.org/10.1103/PhysRevLett.86.3200

34. D. J. Watts, S. H. Strogatz, Collective dynamics of 'small-world' networks, *Nature*, **393** (1998), 440–442. https://doi.org/10.1038/30918

35. M. Sgandurra, L. Muñoz-González, R. Mohsen, E. C. Lupu, Automated dynamic analysis of ransomware: Benefits, limitations, and use for detection, (2016), arXiv:1609.03020. https://doi.org/10.48550/arXiv.1609.03020

36. Y. Ye, T. Li, D. Adjeroh, S.S. Iyengar, A survey on malware detection using data mining techniques, *ACM Comput. Surv.*, **50** (2017), 41. https://doi.org/10.1145/3073559

37. Z. F. Wang, X. Q. Nie, M. X. Liao, Stability analysis of a fractional-order SEIR-KS computer virus-spreading model with two delays, *J. Math.*, **2021** (2021), 6144953. https://doi.org/10.1155/2021/6144953

38. L. J. Yang, Q. K. Song, Y. R. Liu, Dynamics analysis of a new fractional-order SVEIR-KS model for computer virus propagation: Stability and Hopf bifurcation, *Neurocomputing*, **598** (2024), 128075. https://doi.org/10.1016/j.neucom.2024.128075

39. M. Wang, Y. R. Wang, R. Chu, Dynamical analysis of the incommensurate fractional-order Hopfield neural network system and its digital circuit realization, *Fractal Fract.*, **7** (2023), 474. https://doi.org/10.3390/fractalfract7060474

40. M. Abu Hammad, I. Zouak, A. Ouannas, G. Grassi, Fractional discrete computer virus system: chaos and complexity algorithms, *Algorithms*, **18** (2025), 444. https://doi.org/10.3390/a18070444

41. S. Gao, H. H. Iu, U. Erkan, C. Simsek, A. Toktas, Y. H. Cao, A 3D memristive cubic map With dual discrete memristors: design, implementation, and application in image encryption, *IEEE T. Circ. Syst. Vid.*, **35** (2025), 7706–7718. https://doi.org/10.1109/TCSVT.2025.3545868

42. S. Gao, Z. Y. Zhang, H. H. Iu, S. Q. Ding, J. Mou, U. Erkan, A parallel color image encryption algorithm based on a 2-D Logistic-Rulkov nuron map, *IEEE Internet Things*, **12** (2025), 18115–18124. https://doi.org/10.1109/JIOT.2025.3540097

43. F. M. Atici, P. W. Eloe, Discrete fractional calculus with the nabla operator, *Electron. J. Qual. Theory Differ. Equ.*, **2009** (2009), 1–12. https://doi.org/10.14232/ejqtde.2009.4.3

44. T. Abdeljawad, On Riemann and Caputo fractional differences, *Comput. Math. Appl.*, **62** (2011), 1602–1611. https://doi.org/10.1016/j.camwa.2011.03.036

45. G. A. Anastassiou, Principles of delta fractional calculus on time scales and inequalities, *Math. Comput. Model.*, **52** (2010), 556–566. https://doi.org/10.1016/j.mcm.2010.03.055

46. M. T. Shatnawi, N. Djenina, A. Ouannas, I. M. Batiha, G. Grassi, Novel convenient conditions for the stability of nonlinear incommensurate fractional-order difference systems, *Alex. Eng. J.*, **61** (2022), 1655–1663. https://doi.org/10.1016/j.aej.2021.06.073

47. M. A. Ansari, D. Arora, S. P. Ansari, Chaos control and synchronization of fractional order delay-varying computer virus propagation model, *Math. Method. Appl. Sci.*, **39** (2016), 1197–1205. https://doi.org/10.1002/mma.3565

48. G.-C. Wu, D. Baleanu, Jacobian matrix algorithm for Lyapunov exponents of the discrete fractional maps, *Commun. Nonlinear Sci.*, **22** (2015), 95–100. https://doi.org/10.1016/j.cnsns.2014.06.042

49. S. Gao, S. Q. Ding, H. H.-C. Iu, U. Erkan, A. Toktas, C. Şimşek, et al., A three-dimensional memristor-based hyperchaotic map for pseudorandom number generation and multi-image encryption, *Chaos*, **35** (2025), 073119. https://doi.org/10.1063/5.0270220

AIMS Press